Diyala Journal of Engineering Sciences

ISSN 1999-8716

Printed in Iraq

First Engineering Scientific Conference
College of Engineering –University of Diyala
22-23 December. 2010, pp. 92-115

THE EFFECT OF FUEL WITH ADDITIVES ON THE VIBRATION DYNAMIC RESPONSE OF IC ENGINE

Mauwafak Ali Tawfik, Adel Mahmoud Saleh and Hassan Mansour Raheem
Mechanical Department , University of Technology

ABSTRACT:- This study targets at finding the effects of methanol blending to gasoline on dynamic response of IC engine. The fuel blends were prepared by blending 0, 10 and 20 vol. % of methanol with a specified amount of gasoline. These fuel blends were designated as M0G100, M10G90 and M20G80, respectively. Base commercial gasoline (Octane No. is 81) was used in this study. The experiments were conducted on a single cylinder, four stroke variable compression “Varicomp” Dual Diesel /Petrol cycles with a dynamometric test unit type (GR0306/000/037A Prodit) under various engine speeds 1200 RPM up 2000 RPM for increment of 400 RPM at constant torque of (10 N.M), and compression ratio is 9 .The data acquired from these experiments present the relation between the cylinder pressure and the crank angle.

For the purpose of investigating the vibration response of IC engine under dynamically loaded and ignition condition, the experimented cylinder pressure profiles of (Prodit) single cylinder four stroke engine for different percentage of methanol blending with gasoline base fuel, was assumed to be created in each cylinder of (Zetor-M-Type) in-line four cylinder-four stroke engine. Transfer matrix method (TMM) was adopted to calculate the vibration of the crankshaft for the latter engine. It is accounted for the shear effect and gyroscopic effect for the mathematical model of the crankshaft and the effect of unbalance forces, Also it's accounted for the dynamic loads that are applied on main and big end bearings , and two coefficients of damping and stiffness represented the oil film for each bearing.

To embrace the theoretical side, a computer program (Fortran 90), which depends on the data acquired from the experimented work, is constructed to compute the vibration response along the crankshaft of engine for each fuel (M0G100, M10G90, M20G80) to

compare the vibration for each case of cited mixture of fuel and to get the suitable fuel for engine.

The result of this study showed that the M10G90 yields the best fuel for engine to get better vibration then M0G100 and M20G80.

Keywords:- Internal combustion engine, crankshaft, vibration, gasoline, transfer matrix method.

NOMENCLTURE

Symbol	Meaning	Unit
A	Accelration of engin piston	m/s^2
R	Radius of the crankshaft	m
l	Length of connected rod	m
D	Diameter of piston	m
F_x , F_y	The component of external forces acting on crankshaft	N
R_x , R_y	The component of rection at main bearings	N
$[F]$	Field matrix	
$[P]$	Point matrix	
$\overline{Z}$	State vector in complex state	
Z	State vector	
X , Y , Z	Components of amplitude in x, y and z direction respectivly	
ϕ_z, ϕ_y, ϕ_x	Slop in x, y and z axis	degree
V_z, V_x, V_y	Components of inertial shear force in x, y and z direction respectivly	N
M_z, M_x, M_y	Components of bending moment in x, y and z direction respectivly	N.m
V_{az}, V_{ax}, V_{ay}	External shear force	N
M_{az}, M_{ax}, M_{ay}	External bending moment	N.m
$[R]$	Transformation matrix	
U_y^* U_x^*	Components of unbalance force	N
I_z, I_x, I_y	Moment of inertia in x, y and z direction respectivly	$Kg.m^2$
J_z, J_x, J_y	Second moment of area in x, y and z direction respectivly	m^4
θ	Rotation angle for crankshaft	degree
Ω	Rotation speed	r.p.m
χ	Shape Factor	
L_i	Length of the element	m
M_p	Piston mass	Kg

M_g	Gudgeon pin mass	Kg
m_{px} , m_{py}	Mass of support strcture of bearings	Kg
m_r	Partial mass of conectted rod connecte with crankshaft	Kg
m_i	Mass at station 'i'	Kg
K_{xx} , K_{yy}	Stiffness coefficient of bearings	N/m
K_x , K_y	Stiffness coefficient of support at main bearings	N/m
D_{xx} , D_{yy}	damping coefficient of bearings	N.s/m
D_x , D_y	Damping coefficient of support at main bearings	N.s/m
T.D.C	Top Dead Center	
Subscripts		
i	Index of the i^{th} station of the system	
x , y , z	Refer to the parameter in x, y and z direction	
a	Refer to the external parameter	
Superscripts		
L	Refer to parameter of the state vector just to the left of a crankshaft station	
R	Refer to parameter of the state vector just to the right of a crankshaft station	
r	Refer to the real part of the parametre considered	
i	Refer to the imanginary part of the parametre considered	

1. INTRODUCTION

The internal combustion engine are the driving force in most today's automotive applications in these engines ,the combustion of a mixture of air and fuel takes place in a confined area called the combustion chamber. Heat energy is released as a result of the oxidation of fuel molecules during the combustion process. The released heat energy causes the combustion gases to expand forcing the piston downward and thus exerting a rotational force on the crankshaft of the engine (1).

The commencement of the combustion process is triggered either by an external spark as in the case of spark-ignition (SI) engines or by the injection of the fuel into a highly compressed air as in the case of compression –ignition (CI) engines. Figure (1) shows the basic structure of a spark-ignition engine (2, 3).

The literature review related to the subject of the research deals with the studies of the effect and behavior of IC engine due to additives with fuel, also the studies related to the vibration in crankshaft of IC engine as a main part of the engine and the method of the analysis. Robert S. Lunt (4), studied the effect of fuel type on the emission of the IC engine by doing experiments on many types of cars using methanol gasoline fuel and compared the results. The results showed when blended (15% Vol.) methanol with gasoline reduce the

(CO) concentration of exhausted gases also (NO_x) concentration was reduced due to high evaporation temperature of methanol that's lead to reduce the high flame temperature .

Holger Menrad [5], studied the effect blending alcohol with gasoline on the Reid Vapor Pressure (RVP) of the mixture. The results showed RVP of mixture is increasing when alcohol add to gasoline and this rate of increasing depend on the RVP of gasoline and the percentage of added of methanol, also the researchers observed when the methanol additives as (20% Vol.) to gasoline that's produce to reduce the RVP of mixture less than RVP of gasoline alone.

S.M. Fayyad [6], this research presented an investigation of the effects of ethanol addition to low octane number gasoline, on the fuel octane number and on the performance of the engine. In this study, the tested gasoline (octane number = 90) is blended with five different percentages of ethanol, namely 3, 6, 9, 12 and 15% on volume basis. Then these fuel blends, as well as the base gasoline fuel, were burnt in the tested engine. It is found that the octane number of gasoline increases continuously and linearly with increasing the ethanol percentage in gasoline. Hence, ethanol is an effective compound for increasing the value of the octane number of gasoline. Also, it is also noticed that the best performance of the engine was obtained when 15% of ethanol was used in the gasoline blend.

Researcher studied blending alcohol with fuel by focusing on the emissions gases and as overall performance of the engine excluding the analysis the effect of blending on the vibration of engine. Tawfik M.A.[7] , developed a mathematical model of the crankshaft of the 4-cylinder four-stroke engine, the study include a comprehensive analysis of the performance of the crankshaft under misalignment condition, the researcher was adopted the mathematical model on the beam theory ,also the transfer matrix method was used to analyze the vibration of the crankshaft. Also the effects of the gyroscope and the unbalance forces were catered for. A. Suhail [8],studied the dynamic respond of the camshaft using transfer matrix method and found that increasing the number of camshaft affects the rotor gives critical speed lower as well as to reduce the rotor diameter lead to decrease critical speed compared to the rotor has greater diameter , also noted that the number of bearings affect the critical speed where reduce the number of bearings critical speed decrease also, he observed that the amount of force on the surface of the cam depends on the speed of rotation and angle of cam. It can be observed from the previous studies a Transfer Matrix Method (TMM) is identified as one of the effective methods developed to deal with vibration problem. The basic philosophy adopted in this method is based on the idea of breaking up a complicated system into component parts with simple elastic and dynamic properties that can readily be expressed in matrix form to solve the problem of the system. This study was motivated by a need for a comparative study of gasoline fuel and Additives of fuel to get the suitable operation of engine such as low vibration used an automotive to specify the optimum operating condition for the IC engine.

2. THEORETICAL ANALYSIS

Crankshaft is a large component with a complex geometry in the engine, which converts the reciprocating displacement of the piston to a rotary motion [9] ,TMM was used to calculate the vibration of the crankshaft of IC engine, the analyzes of crankshaft have steps as bellow:

2.1 Determination the Dynamic Forces on the Crankshaft and Reactions at Main Bearings

2.1.1 Determination the Forces at the Big-End of Connected Rod

Figure (2) represents the mechanism of the crankshaft, connecting rod and piston of the reciprocation engine, the acceleration of the piston can be calculated according to equation (1)[10].

$$A = R\omega^2 \left\{ \cos\theta + \left[\left(q^2 - 1\right)\cos 2\theta + \cos^4\theta \right] / \left(q^2 - \sin^2\theta\right)^{3/2} \right\} \qquad \dots (1)$$

Where:

R: is the radius of crankshaft

q: is the ratio of connected rod length to the crankshaft radius

θ: is the angle of crankshaft

The inertial force of the reciprocating masses F_I (piston, gudgeon pin, and the small end of the connecting rod) is obtained from the following relation:

$$F_I = \left(M_1 + M_P + M_g\right) * A \qquad \dots (2)$$

Where:

M_1: is the" equivalent mass of the small end of the connecting rod, and is usually taken "1/3"of the connecting rod mass [11].

M_P, M_g: are the piston, and gudgeon pin mass respectively.

If P_G is the gas pressure acting upon the piston, the gas force being applied on the piston F_G is:

$$F_G = \left(\pi D^2 / 4\right) * P_G \quad \ldots (3)$$

Where:

D: is the piston diameter.

So that F_1 will be:

$$F_1 = \left(F_G - F_I\right) * \sec\phi \quad \ldots (4)$$

A centrifugal force F_2 experienced by the connected rod mass associated with the crank pin may be written as:

$$F_2 = M_2 R \omega^2 \quad \ldots (5)$$

Where:

M_2: is taken "2/3" of the total connecting rod mass [11].

Thus, resultant forces in 'x' and 'y' direction acting upon the crank pin are:

$$\left.\begin{aligned} F_X &= F_2 \sin\theta + F_1 \sin\phi \\ F_Y &= F_1 \cos\phi - F_2 \cos\theta \end{aligned}\right\} \quad \ldots (6)$$

2.1.2 Determination the Reaction at the Main Bearing

External load on the main bearings may be calculated by considering the crankshaft as statically indeterminate beam with multi support at each main bearing and by assuming constant distance between two supports and the geometry and properties for two each support. Figure (3) shows elastic beam under dynamic forces [11] were calculated before, and from the bending moment diagram and the elastic beam diagram, it have got three equation including the moment for each span and (F_{Yi}) by solving this equations and doing equilibrium for each span of elastic beam that lead to calculate the reaction of main bearing.

A computer program has been developed to calculate the reactions at the main bearings of the crankshaft for (Line Type) and any number of cylinders engine.

3. CALCULATION COEFFICIENTS OF JOURNAL BEARINGS

Bearings are under dynamic loading lead to dynamic forces are instantaneously various in the amount and the direction at any time, and thereby change the oil pressure in the bearings as a result of the impact of each of the (wedge, squeezing & whirling).

At any time, the external applied force on each bearing met with a hydrodynamic internal force generate within oil film of bearing, where it is the expression by a four coefficients of springs and dampers in x and y direction propagated balance of the external forces, which is equal to the forces of reaction value and opposite in direction.

Finite difference method is used to solve the Reynolds equation [7] ,and then finding the load carrying capacity in two components. The radial load (W_R) which is the sum of the load components along the line of center, and the tangential load (W_T) which is the sum of the load components perpendicular to the line of centers [13].

$$\frac{\partial}{\partial x}\left(\frac{\rho_{oil} * h^3}{12\eta_{oil}}\frac{\partial P}{\partial x}\right)+\frac{\partial}{\partial z}\left(\frac{\rho_{oil} * h^3}{12\eta_{oil}}\frac{\partial P}{\partial z}\right)=\frac{\partial}{\partial x}\left(\rho_{oil}\frac{U_o+U_h}{2}h\right)+\rho_{oil}\frac{\partial h}{\partial t} \qquad \text{... (7)}$$

The radial load is given by:

$$\overline{W}_R = 2\pi\int_{-1/2}^{1/2}\int_0^1 -\overline{P}\cos\phi dxdz \qquad \text{… (8)}$$

And the tangential load is given by:

$$\overline{W}_T = 2\pi\int_{-1/2}^{1/2}\int_0^1 \overline{P}\sin\phi dxdz \qquad \text{… (9)}$$

Thus, the load carrying capacities are equal to the radial and tangential oil film forces (F_R) and (F_T) respectively, taking into account the sign convention:

$$\left.\begin{aligned}\overline{F}_R &= -\overline{W}_R\\ \overline{F}_T &= \overline{W}_T\end{aligned}\right\} \qquad \text{… (10)}$$

And by writing the equations of radial and tangent oil film forces in both directions x and y results in the following:

$$\left.\begin{aligned}\overline{F}_X &= \overline{F}_R\sin\beta+\overline{F}_T\cos\beta\\ \overline{F}_Y &= \overline{F}_R\cos\beta-\overline{F}_T\sin\beta\end{aligned}\right\} \qquad \text{… (11)}$$

As shown in Figure (4), it can be written as follows:

$$\left.\begin{aligned}x &= c\varepsilon\sin\beta\\ y &= c\varepsilon\cos\beta\end{aligned}\right\} \qquad \text{… (12)}$$

By making use of equations (11) and (12) , and considering the squeezing , whirling and wedge action, the stiffness and damping coefficients can be calculated at any instant of time by method (Euler - Cauchy Time Marching Scheme) [7]. A program has been developed to calculate the characteristic coefficients of the oil film of the bearing.

4. CALCULATION THE DYNAMIC RESPONSE OF THE CRANKSHAFT

A 3-dimensional analysis is considered for the crankshaft, also represented by using the Transfer Matrix Method (TMM). It is adopted in this analysis where the solution of the crankshaft section is represented by a field matrix (a beam element matrix) [F] which relates the state vectors at the ends of any crankshaft station (13). At each section there is a point matrix (a mass element matrix) [p] which relates the state vectors to the left and right of any station "i". As shown in Figure (5).

4.1 Point Matrix

There are five cases for the point matrix to be consider theses cases cover all possible arrangement at any station along the crankshaft. The cases are:

1. lumped masses element
2. Pully or flywheel
3. Main bearing
4. Big-end beraing
5. Branch of counter weight

Case-1 Point matrix of lumped mass element at station"i"

In general its assumed that positive boundery at (right of station "i") the internal forces and moments will considerd positive in the direction of coordinate and negative at boundery (left of station "i") pointing to the negative direction of the coordinates. From figure (6) the equliburim equation of mass (m_i) in three dimension (z, x and y) respectively gives the point matrix as shwon in Figure (7)**.**

Case -2 Point matrix of pully or flywheel at station"i"

This case doesn't differe from the case of lumped mass according to the slop, shear force, moment and deflection at the right and left of station.

Case -3 Point matrix of Main bearing at station"i"

Figure (8) represents a mathematical model of main bearing; K_{xx}, K_{yy} are the spring coefficients and D_{xx}, D_{yy} are the damping coefficients of the bearing in x-y direction.

The supporting structure is replace by four coefficients K_x and K_y are the two spring coefficients, Dx and D_y are the two damping coefficients of the supporting structure (7).

By and considering the equilibrium of forces in y and x direction of mass (m_i) gives the point matrix as shwon in figure (9).in case of main bearing the values of (FX & FY) equle to zero and the value of a_1 and a_2 as shwon:

$$a_1 = \frac{\left[(m_{Px}\Omega^2 - K_X) - j\Omega D_X\right]\left[K_{XX} + j\Omega D_{XX}\right]}{(m_{Px}\Omega^2 - K_{XX} - K_X) - j\Omega(D_{XX} + D_X)}$$

$$a_2 = \frac{\left[(m_{Py}\Omega^2 - K_Y) - j\Omega D_Y\right]\left[K_{YY} + j\Omega D_{YY}\right]}{(m_{Py}\Omega^2 - K_{YY} - K_Y) - j\Omega(D_{YY} + D_Y)}$$

Case-4 Point matrix of big-end bearing at station"i"

As shwon in figure (10), point load and external load are considered. In addition to, the flexible oil film are represented as damping and stifness coefficient. By considering the equilibrium of forces in y and x direction, also by considering the equilibrium of forces in y and x direction of mass (m_i) gives the point matrix as shwon in figure (11). In case of main bearing the values of (FX & FY) equle to external load and the value of a_1 and a_2 as shwon:

$$a_1 = \frac{\left[K_{XX} + j\Omega D_{XX}\right]}{(m_r\Omega^2 - K_{XX}) - j\Omega D_{XX}}$$

$$a_2 = \frac{\left[K_{YY} + j\Omega D_{YY}\right]}{(m_r\Omega^2 - K_{YY}) - j\Omega D_{YY}}$$

Case-5 Point matrix of branch of counter weight at station"i"

Referring to figure(12), and assuming the transfer matrix after multiplucation of field and point matrices is [U], the transfer matrix relation between the two ends of freed branched parts of structure will be as follow [7]:

$$\begin{bmatrix} Q \\ \cdots \\ R \\ \cdots \\ 1 \end{bmatrix}^K = \left[\begin{array}{c|c|c} U_{VV} & U_{VP} & U_V \\ \hline U_{PV} & U_{PP} & U_P \\ \hline 0 & 0 & 1 \end{array}\right]^O \begin{bmatrix} Q \\ \cdots \\ R \\ \cdots \\ 1 \end{bmatrix}^O \qquad \ldots(13)$$

Where:

$$Q = \{Z, X, Y, \phi_Z, \phi_X, \phi_Y\}$$

$$R = \{V_Z, V_X, V_Y, M_Z, M_X, M_Y\}$$

Then apply boundery condition (R=0) and transfer the coordnete of branch to main system cordinate, gives the point matrix of this case as shown in figrue (13).

5. FIELD MATRIX (ELEMENT MATRIX)

Consider the massless beam element between station "i" and "i-1", the matrix connected the right state vector of (m_{i-1}) and the left state vector of (m_i) called field matrix, In order to determine the field matrix of any beam elements arbitrary orientation in space, apportion of massless beam must be considered in z-y and z-x plans as shown in figures (14), (15) and (16). By doing equilibrium equations for these figures and taking into account the effect of shear force and slope, gives the field matrix for system as shown in figure (17).

It can be observed the point matrix in cases of lumped mass, main and big-end bearing matrix are complex, it's have real and imaginary elements, so to achieve the calculation matrices must be splitted to real and imaginary parts[7]. For calculating the state vector at any station "i" in terms of state vector at the boundary written as follows [14]:

$$\{Z\}_n^R = [P]_n [F]_{n-1} [P]_{n-1} \quad ....[F]_2 [P]_2 [F]_1 [P]_1 \ \{Z\}_1^L \qquad ...(14)$$

A computer program has been developed to calculate the deflection, shear force, bending moment and slop at each station along the crankshaft.

6. EXPERIMENTAL TEST FACILITY

Experiments were carried out on a single-cylinder variable compression ICE “varicomp” Dual Diesel /Petrol cycles with Dynamometric test unit “type (GR0306/000/037A) Prodit company, (Italy)[15], Specifications of the engine are shown in Table 1. The engine was fuelled with gasoline fuel (ON 81) then, The engine was operated at 1200 RPM to 2000 RPM with an increment of 400 RPM and loaded by hydraulic dynamometer at 10 N.m for each operation speed and mixture of fuel (M0G100, M10G90 and M20G80). The relation between cylinder pressure and crank angle was acquired from interface for each case of mixture.

To embrace the theoretical side, a computer program (FORTRAN 90), which depends on the data acquired from the experimented work, is constructed to compute the vibration response of the engine using gasoline fuel with different additives and then to study the effect of the implementation such fuel on the dynamic response of the engine.

7. RESULTS AND DISCUSSION

For the purpose of investigating the vibration response of IC engine under dynamically loaded and ignition condition, the experimented cylinder pressure profiles of

(Prodit) single cylinder four stroke engine for different percentage of methanol blending with gasoline base fuel, was assumed to be created in each cylinder of (Zetor-M-Type) in-line four cylinder-four stroke engine (since the data and dimensions of the latter engine are available). The zetor engine has firing order of (1-3-4-2).

The amplitudes along the crankshaft are investigated due to the implementation of blending methanol with gasoline (base fuel) at different volumetric percentage of methanol (0, 10 and 20 % vol.,) respectively in IC engine.

Figures (18), (19) and (20) show three dimensional view of the amplitude along the stations of the crankshaft for different speeds (1200, 1600 and 2000 RPM) and different percentage of methanol to be blended with the bas fuel (gasoline).

In general, it is obvious from these figures, using different percentage of blended methanol affect the dynamic response of the engine. Also, it is clear that the deflection at over hanged crankshaft stations are greater than the other crankshaft stations due to the inertia effect of the flywheel and pulley at the tip ends. Mostly the action of firing order can be also distinguished as peaks from the cited figures.

Also, it can be seen from those figures the least behavior of amplitude is at (M10G90) compared with (M0G100) and (M20G80) at speeds (1200, 1600 and 2000 RPM), this may be related to the fact that (RVP) for the mixture of the blended methanol with gasoline less than that of the base fuel at 20% and above which in turned decreasing the efficiency of the mixture combustion in the cylinder [(5)].

In addition to that as methanol percent increases in mixture the rate of unburned hydrocarbons will be increased so that the vibration will be increased too.

It can be seen from figures (21), (22) and (23) the amplitude along the crankshaft at different speeds (1200, 1600 and 2000 RPM) at the big-end bearing stations are higher than those at main bearing stations due to the effect of forces gas cylinder pressure and inertia. Also it's obvious that the vibration along crankshaft again at (M10G90) is less than that of (M0G100) and (M20G80) for all the different speeds.

8. CONCLUSIONS

Using different percentage of blended methanol with gasoline was affecting on the dynamic response of the engine. Also, it is clear that the deflection at over hanged crankshaft stations are greater than the other crankshaft stations due to the inertia effect of the flywheel and pulley at the tip ends.

Also, it can be seen from this study the least behavior of amplitude is at (M10G90) compared with (M0G100) and (M20G80) at speeds (1200, 1600 and 2000 RPM) and the amplitude along the crankshaft at the big-end bearing stations are higher than those at main bearing stations due to the effect of forces gas.

REFERENCES

1. Stephen, R, T, (2000), "An Introduction to Combustion Concepts and Applications", McGraw-Hill, Second edition.
2. Heywood, J, B, (1988), "Internal Combustion Engine Fundamental," McGraw-Hill.
3. Taylor, C, F, (1985), "The Internal Combustion Engines in Theory and Practice "Volume 1 &2, MIT press, second edition.
4. Robert, S, L, & Eric, E, W, (1974), "Methanol as a Gasoline Extender-Fuel Economy Emissions and High Temperature Drivability" S.A.E. Paper No.741008.
5. Holger , M, & Bernd, N, (1980), "Engine and Vehicle Concepts for Methanol – Gasoline Blends" , S.A.E. Paper No.831686.
6. Fayyad, S, M, Waleed, M, Abu-Ein ,S, Q,Juditawy,O, and Abu-Rahmeh , T, (2010), " Experimental Investigation of Using Fuel Additives – Alcohol" Research Journal of Applied Sciences, Engineering and Technology 2(2): 164-169.
7. Tawfik , M ,A., (1996)," The effect of misalignment on the dynamic performance of crankshaft bearing system in a diesel engine ", Ph.D. Thesis, Mechanical engineering, University of Technology.
8. Pestel ,E,L, & Leckie, F,A, (1963), "Matrix Method in Elasto Mechanics", McGrow Hill, New York.
9. Farzin, H, and Ali, F,,(2007)," Stress Analysis and Optimization of Crankshafts Subject to Dynamic Loading, The University of Toledo.
10. Shaw ,M,C, and Macks, F, (1949), "Analysis and Lubrication of Bearing" McGraw Hill Newyork .
11. Garner, A , (1982), "Elements Of Mechanics Of Materials" , Prentice-Hall .
12. Safar,Z, Elkotb,M, and Mokhtar, DM , (1989)," analysis of Misaligned Journal Bearing Opertion in Turbulent Regime" transction of the ASME ,journal of tribology , pp. (215-219).
13. Alaa, A. J., (2008),"Vibration Analysis of Simple Home Generator"", M.Sc. Thesis, Mechanical engineering, University of Technology.

14. Rahnejat, H. and Gohar, R, (1985), "The vibrations of radial ball bearings. Proc. Inst. Mech. Eng. [C] , 199(C3), 181-193.
15. Prodit Engineering company, (2004), "Instruction Manual, Variable Compression Engine "VARICOMP" Dual Diesel/Petrol Cycle with Dynamometric Test Unit".

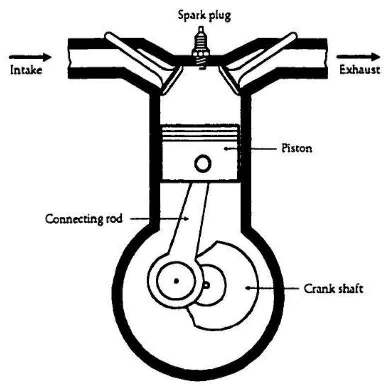

Fig. (1): The basic structure of a spark-ignition engine.

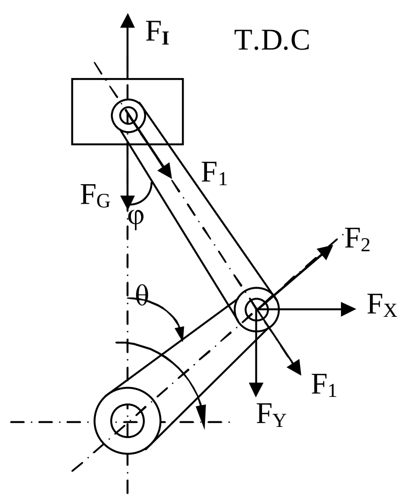

Fig.(2): The Mechanism of The Crankshaft, Connecting Rod and Piston.

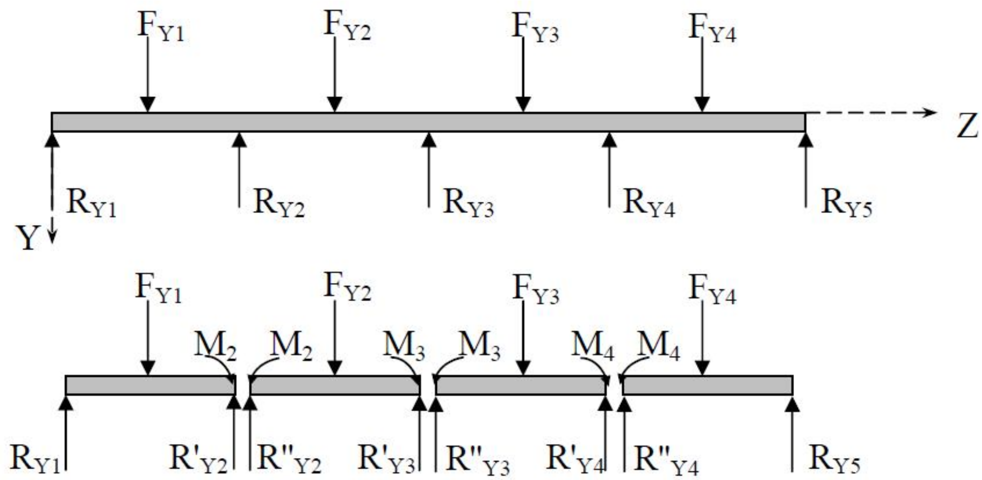

Fig. (3): Analysis of elastic beam under dynamic forces.

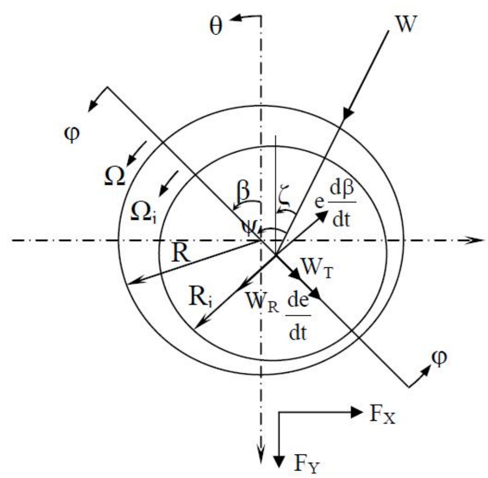

Fig. (4): Journal bearing.

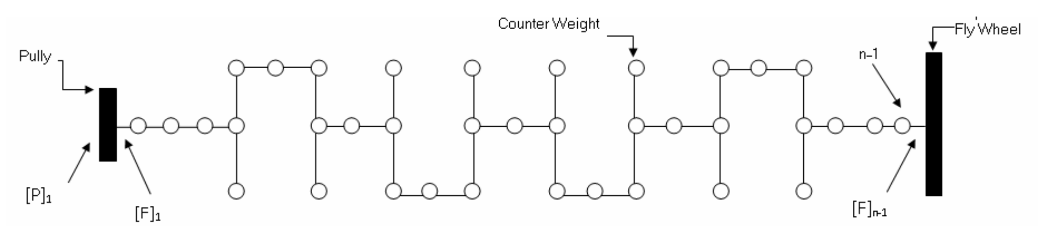

Fig. (5): Theoretical Model of Crankshaft System.

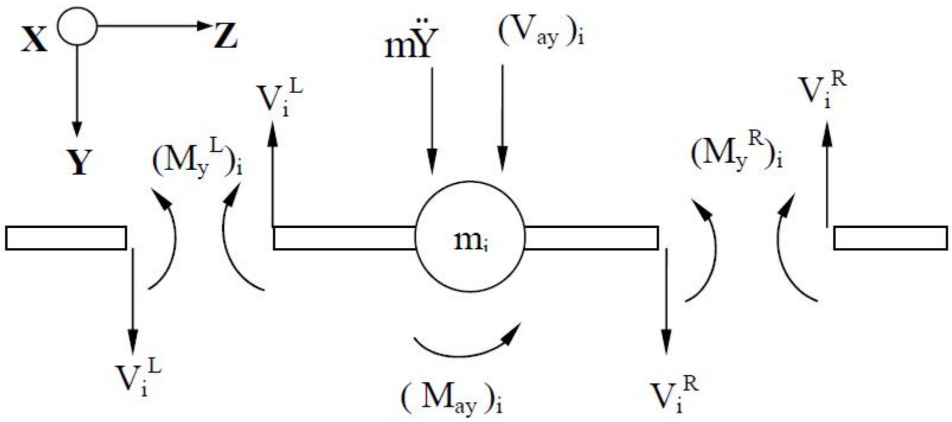

Fig. (6): Free body digram of lumped masses**.**

$$
\begin{bmatrix} \bar{Z} \\ \bar{X} \\ \bar{Y} \\ \bar{\phi}_z \\ \bar{\phi}_x \\ \bar{\phi}_y \\ \bar{V}_z \\ \bar{V}_x \\ \bar{V}_y \\ \bar{M}_z \\ \bar{M}_x \\ \bar{M}_y \\ 1 \end{bmatrix}_i^R
=
\left[\begin{array}{ccc|ccc|ccc|ccc|c}
 & & & & & & & & & & & & 0 \\
 & [E] & & & [0] & & & [0] & & & [0] & & 0 \\
 & & & & & & & & & & & & 0 \\
\hline
 & & & & & & & & & & & & 0 \\
 & [0] & & & [E] & & & [0] & & & [0] & & 0 \\
 & & & & & & & & & & & & 0 \\
\hline
-m\Omega^2 & 0 & 0 & & & & & & & & & & -V_{az} \\
0 & -m\Omega^2 & 0 & & [0] & & & [E] & & & [0] & & -V_{ax} \\
0 & 0 & -m\Omega^2 & & & & & & & & & & -V_{ay} \\
\hline
 & & & -\Omega^2 I_z & 0 & 0 & & & & & & & -M_{az} \\
 & [0] & & 0 & -\Omega^2 I_x & j\Omega^2\Delta I & & [0] & & & [E] & & -M_{ax} \\
 & & & 0 & -j\Omega^2\Delta I & -\Omega^2 I_y & & & & & & & -M_{ay} \\
\hline
0 & 0 & 0 & 0 & 0 & 0 & 0 & 0 & 0 & 0 & 0 & 0 & 1
\end{array}\right]
\begin{bmatrix} \bar{Z} \\ \bar{X} \\ \bar{Y} \\ \bar{\phi}_Z \\ \bar{\phi}_X \\ \bar{\phi}_Y \\ \bar{V}_Z \\ \bar{V}_X \\ \bar{V}_Y \\ \bar{M}_Z \\ \bar{M}_X \\ \bar{M}_Y \\ 1 \end{bmatrix}_i^L
$$

Fig.(7): point matrix of lumped mass.

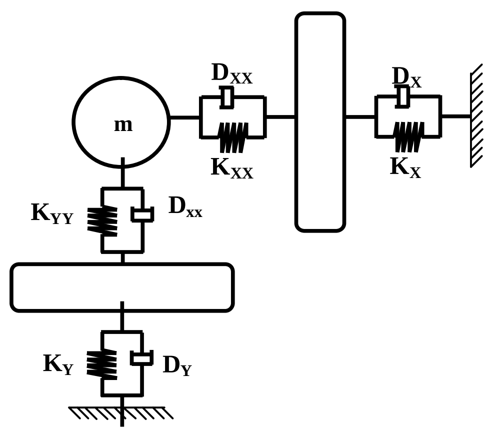

Fig.(8): Mathematical model of main bearing.

$$\begin{bmatrix}\bar{Z}\\ \bar{X}\\ \bar{Y}\\ \bar{\phi}_z\\ \bar{\phi}_x\\ \bar{\phi}_y\\ \bar{V}_z\\ \bar{V}_x\\ \bar{V}_y\\ \bar{M}_z\\ \bar{M}_x\\ \bar{M}_y\\ 1\end{bmatrix}_i^R = \left[\begin{array}{ccc|ccc|ccc|ccc|c} & & & & & & & & & & & & 0\\ & [E] & & & [0] & & & [0] & & & [0] & & 0\\ & & & & & & & & & & & & 0\\ \hline & & & & & & & & & & & & 0\\ & [0] & & & [E] & & & [0] & & & [0] & & 0\\ & & & & & & & & & & & & 0\\ \hline -m\Omega^2 & 0 & 0 & & & & & & & & & & \bar{V}_{az}\\ 0 & a_1-m\Omega^2 & 0 & & [0] & & & [E] & & & [0] & & J\Omega^2\bar{U}-\bar{V}_{ax}\\ 0 & 0 & a_2-m\Omega^2 & & & & & & & & & & -\Omega^2\bar{U}-\bar{V}_{ay}\\ \hline & & & -\Omega^2 I_Z & 0 & 0 & & & & & & & -\bar{M}_{az}\\ & [0] & & 0 & -\Omega^2 I_X & j\Omega^2\Delta I & & [0] & & & [E] & & -\bar{M}_{ax}\\ & & & 0 & -j\Omega^2\Delta I & -\Omega^2 I_y & & & & & & & -\bar{M}_{ay}\\ \hline 0 & 0 & 0 & 0 & 0 & 0 & 0 & 0 & 0 & 0 & 0 & 0 & 1 \end{array}\right] \begin{bmatrix}\bar{Z}\\ \bar{X}\\ \bar{Y}\\ \bar{\phi}_Z\\ \bar{\phi}_X\\ \bar{\phi}_Y\\ \bar{V}_Z\\ \bar{V}_X\\ \bar{V}_Y\\ \bar{M}_Z\\ \bar{M}_X\\ \bar{M}_Y\\ 1\end{bmatrix}_I^I$$

Fig.(9): Point matrix of main bearing.

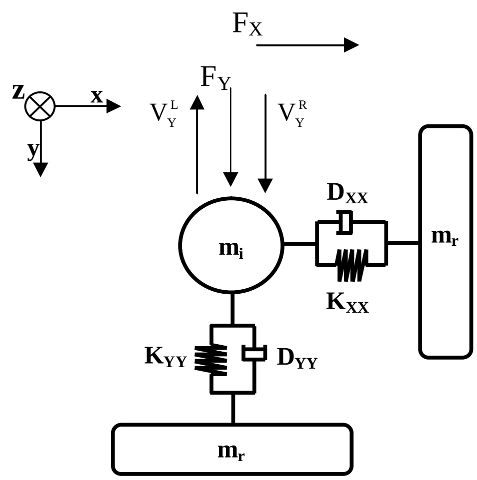

Fig. (10): The mathematical model of the big-end bearing.

$$\begin{bmatrix}\bar{Z}\\ \bar{X}\\ \bar{Y}\\ \bar{\phi}_z\\ \bar{\phi}_x\\ \bar{\phi}_y\\ \bar{V}_z\\ \bar{V}_x\\ \bar{V}_y\\ \bar{M}_z\\ \bar{M}_x\\ \bar{M}_y\\ 1\end{bmatrix}_i^R = \left[\begin{array}{ccc|ccc|ccc|ccc|c} & & & & & & & & & & & & 0\\ & [E] & & & [0] & & & [0] & & & [0] & & 0\\ & & & & & & & & & & & & 0\\ \hline & & & & & & & & & & & & 0\\ & [0] & & & [E] & & & [0] & & & [0] & & 0\\ & & & & & & & & & & & & 0\\ \hline -m\Omega^2 & 0 & 0 & & & & & & & & & & \bar{V}_{az}\\ 0 & a_1-m\Omega^2 & 0 & & [0] & & & [E] & & & [0] & & -F_X+J\Omega^2\bar{U}-\bar{V}_{ax}\\ 0 & 0 & a_2-m\Omega^2 & & & & & & & & & & -F_Y-\Omega^2\bar{U}-\bar{V}_{ay}\\ \hline & & & -\Omega^2 I_Z & 0 & 0 & & & & & & & -\bar{M}_{az}\\ & [0] & & 0 & -\Omega^2 I_X & j\Omega^2\Delta I & & [0] & & & [E] & & -\bar{M}_{ax}\\ & & & 0 & -j\Omega^2\Delta I & -\Omega^2 I_y & & & & & & & -\bar{M}_{ay}\\ \hline 0 & 0 & 0 & 0 & 0 & 0 & 0 & 0 & 0 & 0 & 0 & 0 & 1 \end{array}\right] \begin{bmatrix}\bar{Z}\\ \bar{X}\\ \bar{Y}\\ \bar{\phi}_Z\\ \bar{\phi}_X\\ \bar{\phi}_Y\\ \bar{V}_Z\\ \bar{V}_X\\ \bar{V}_Y\\ \bar{M}_Z\\ \bar{M}_X\\ \bar{M}_Y\\ 1\end{bmatrix}_I^I$$

Fig.(11): Point matrix of big-end bearing.

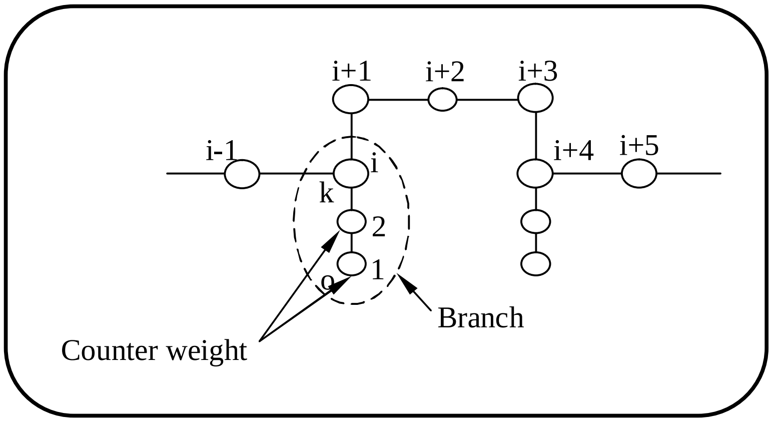

Fig. (12): Model of branch system**.**

$$[P]_i = \left[\begin{array}{ccc:ccc:ccc:ccc:c}
 & [E] & & & [0] & & & [0] & & & [0] & & \begin{matrix}0\\0\\0\end{matrix} \\ \hdashline
 & [0] & & & [E] & & & [0] & & & [0] & & \begin{matrix}0\\0\\0\end{matrix} \\ \hdashline
\multicolumn{6}{c:}{U_{PV}U_{VV}^{-1}} & & \begin{matrix}[E]\\ [0]\end{matrix} & & & \begin{matrix}[0]\\ [E]\end{matrix} & & U_P - U_{PV}U_{VV}^{-1}U_V \\ \hdashline
0 & 0 & 0 & 0 & 0 & 0 & 0 & 0 & 0 & 0 & 0 & 0 & 1
\end{array}\right]$$

Fig.(13): Point matrix of branch**.**

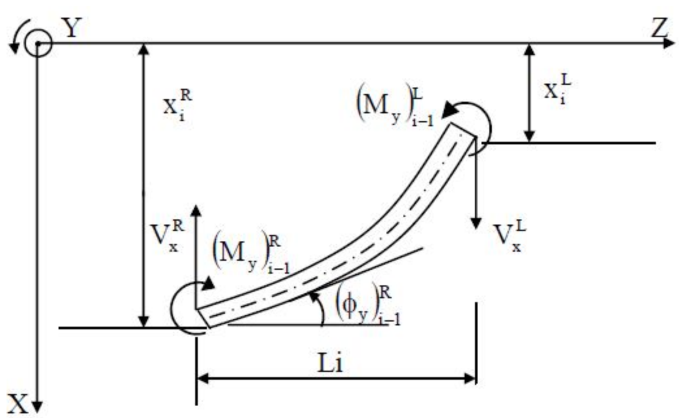

Fig.(14): End forces, moments and deflection for massless beam in z-x plans.

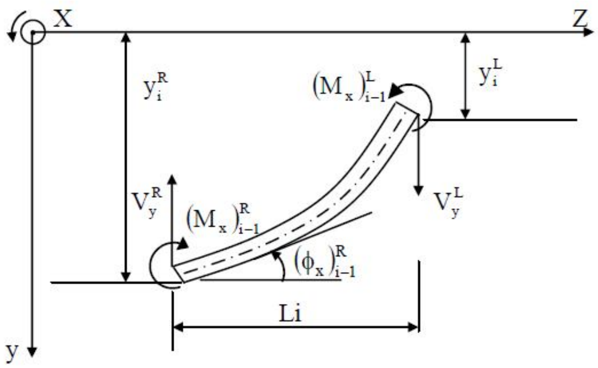

Fig.(15): End forces, moments and deflection for massless beam in z-y plans.

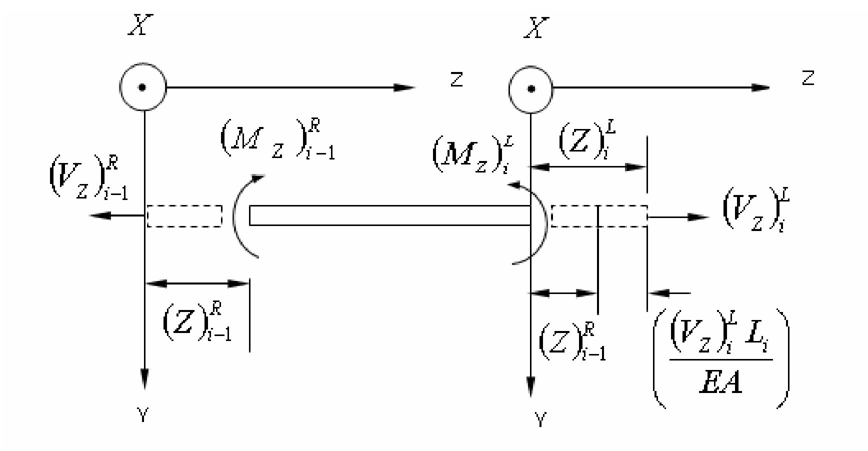

Fig. (16): Beam element under longitudinal vibration**.**

$$
\begin{bmatrix} Z \\ X \\ Y \\ \phi_Z \\ \phi_X \\ \phi_Y \\ V_Z \\ V_X \\ V_Y \\ M_Z \\ M_X \\ M_Y \\ 1 \end{bmatrix}_I^{l}
=
\left[\begin{array}{ccc|ccc|ccc|ccc|c}
 & & & 0 & 0 & 0 & \frac{L}{EA} & 0 & 0 & 0 & 0 & 0 & 0 \\
 & [E] & & 0 & 0 & L & 0 & f_1 & 0 & 0 & 0 & \frac{L^2}{2EJ_X} & 0 \\
 & & & 0 & -L & 0 & 0 & 0 & f_2 & 0 & -\frac{L^2}{2EJ_Y} & 0 & 0 \\
\hline
 & & & & & & 0 & 0 & 0 & \frac{L}{GJ_Z} & 0 & 0 & 0 \\
 & [0] & & & [E] & & 0 & 0 & \frac{L^2}{2EJ_Y} & 0 & \frac{L}{EJ_X} & 0 & 0 \\
 & & & & & & 0 & -\frac{L^2}{2EJ_X} & 0 & 0 & 0 & \frac{L}{EJ_Y} & 0 \\
\hline
 & & & & & & & & & & & & 0 \\
 & [0] & & & [0] & & & [E] & & & [0] & & 0 \\
 & & & & & & & & & & & & 0 \\
\hline
 & & & & & & 0 & 0 & 0 & & & & 0 \\
 & [0] & & & [0] & & 0 & 0 & L & & [E] & & 0 \\
 & & & & & & 0 & -L & 0 & & & & 0 \\
\hline
0 & 0 & 0 & 0 & 0 & 0 & 0 & 0 & 0 & 0 & 0 & 0 & 1
\end{array}\right]
\begin{bmatrix} Z \\ X \\ Y \\ \phi_Z \\ \phi_X \\ \phi_Y \\ V_Z \\ V_X \\ V_Y \\ M_Z \\ M_X \\ M_Y \\ 1 \end{bmatrix}_{I-1}^{R}
$$

Fig.(17): Field matrix

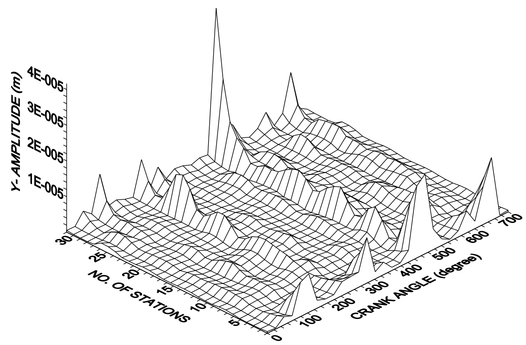

A- M0G100

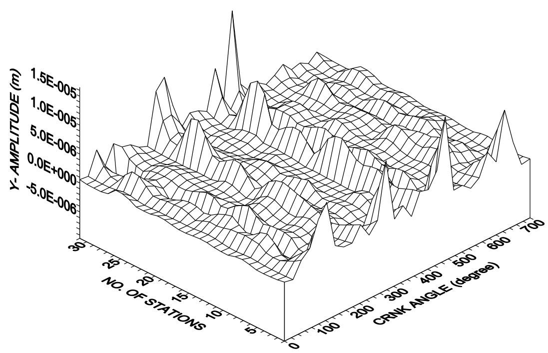

B- M10G90

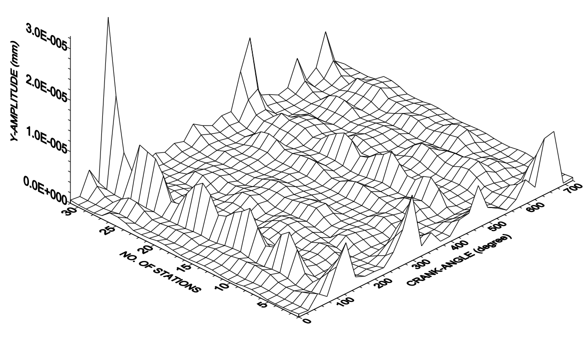

C- M20G80

Fig.(18): The amplitude along crank shaft at 1200 RPM

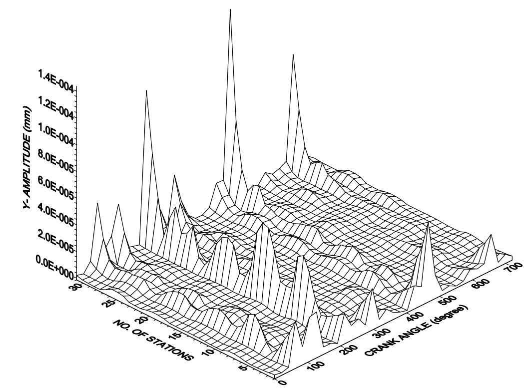

A- M0G100

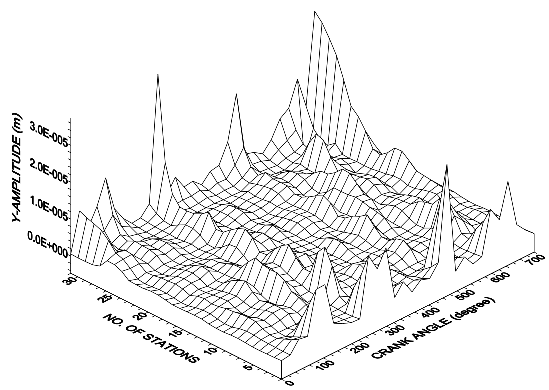

B- M10G90

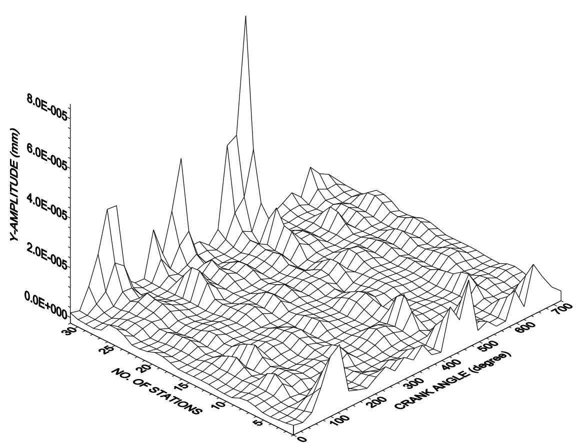

C- M20G80

Fig.(19): The amplitude along crank shaft at 1600 RPM**.**

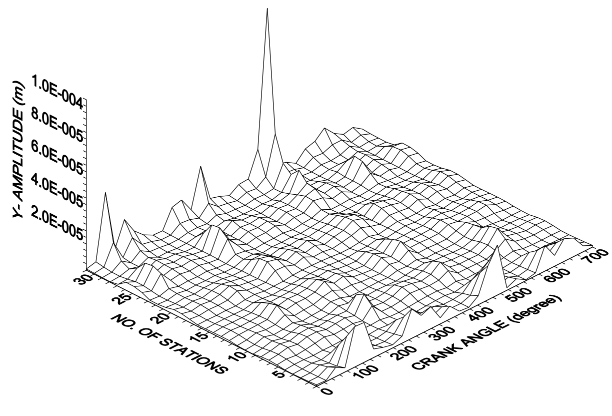

A- M0G100

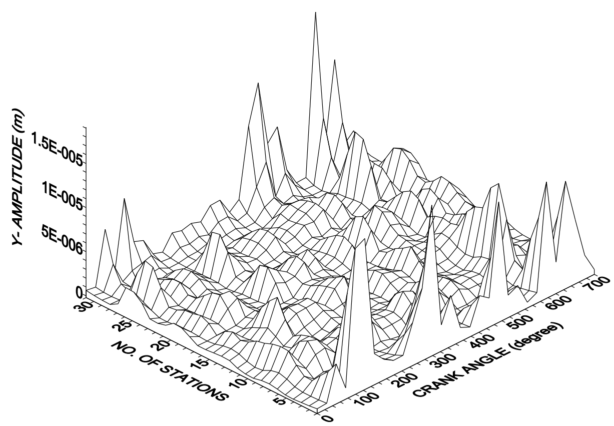

B- M10G90

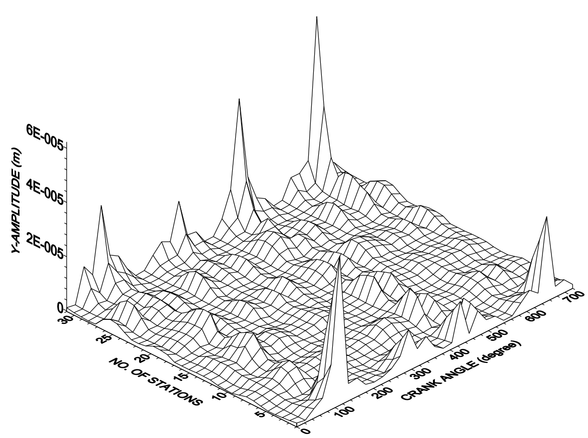

C- M20G80

Fig.(20): The amplitude along crank shaft at 2000 RPM.

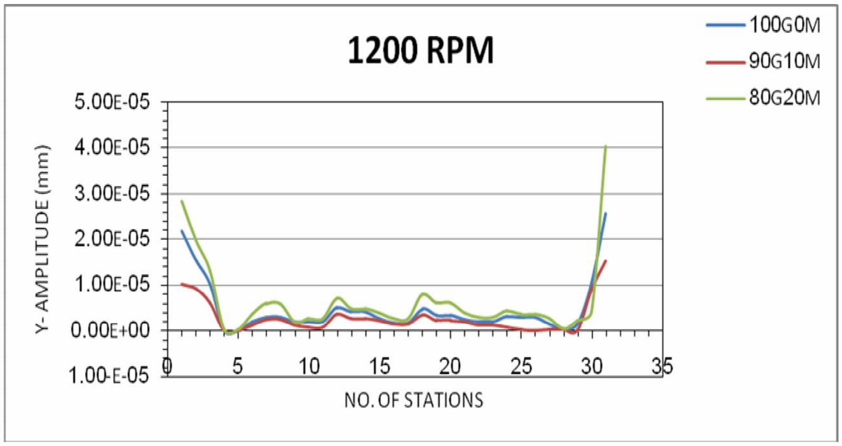

Fig. (21): Y- amplitude at 1200 RPM.

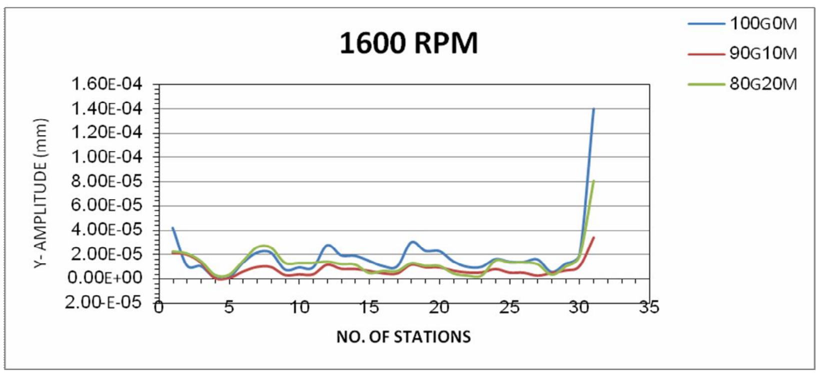

Fig. (22): Y- amplitude at 1600 RPM**.**

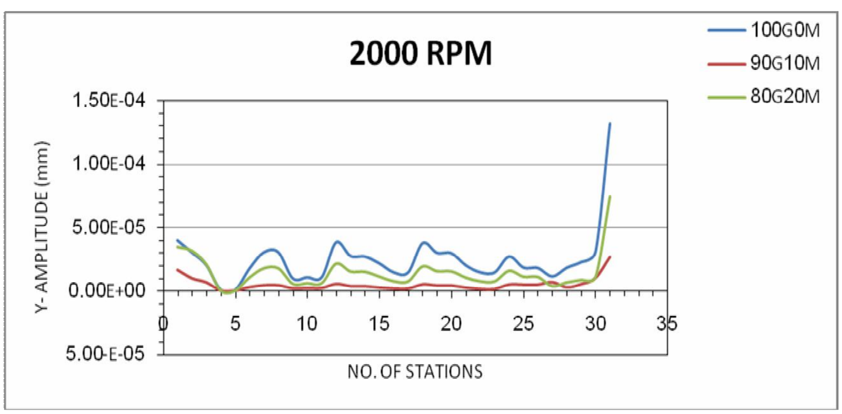

Fig. (23): Y- amplitude at 2000 RPM

Table (1): Properties of Engine.

Internal combustion Engine “Varicomp” Technical characteristics:	
Manufacturer	PRODIT s.a.s.
Cycle	OTTO or DIESEL, four strokes
Number of cylinder	1 vertical
Diameter	90mm
Stroke	85mm
Swept volume	541cm3
Compression ratio	4÷17.5
Max .power	4kWat 2800 rpm
Max .torque	28 Nm at 1600 rpm
Water cooled	
No load speed range	500÷3600 rpm (Otto cycle)
Load speed range	1200÷3600 rpm (Otto cycle)
Intake star	540 before T.D.C
Intake end	220 after T.D.C
Exhaust start	220 before T.D.C
Exhaust end	540 after T.D.C
Fixed spark advance	100 (spark ignition)

تأثير إضافة المحسنات إلى الوقود على الاستجابة الديناميكية لمحركات الاحتراق الداخلي

د.موفق علي توفيق | د.عادل محمود صالح | حسن منصور رحيم
أستاذ مساعد | مدرس | مهندس
الجامعة التكنولوجية- قسم هندسة المكائن والمعدات

الخلاصة

تتضمن هذه الدراسةِ تأثير إضافة الكحول المثيلي (الميثانول) إلى وقود البانزين (الكازولين) على الاستجابة الديناميكية لمحرك احتراق داخلي. إن وقود الكازولين المستعمل في هذه الدراسة هو الوقود التجاري ذو العدد الاوكتاني (81). أجريتْ مجموعة من التجارب في هذه الدراسة على محرك احادي الاسطوانة رباعي الاشواط ذو نسبة انضغاط متغيرة
type (GR0306/000/037A Prodit). "Varicomp" Dual Diesel /Petrol cycles with dynamometric test unit

الاختبارات التي اجريت كانت عند سرع متغيرة ضمن مدى من 1200 الى 2000 (دورة/دقيقة) بزيادة 400 (دورة/دقيقة) وعند نسبة انضغاط 9، وعزم (10 N.m) وباستعمال عدة نسب من خليط الوقود من الكازولين والميثانول (0%،10%، 20%) كنسب حجميه.

البياناتُ التي مثلت الجانب العملي تضمنت العلاقةِ بين الضغطِ في غرفة الاحتراقَ وزاويةَ عمود المرفق. ولغرضِ التحقق من دراسة الاستجابة الديناميكية لمحرك احتراق داخلي يعمل تحت تاثير احمال ديناميكية ونسق اشتعال تم افتراض ان مخطط الضغط في غرفة الاحتراق مع زاوية عمود المرفق الذي استحصل من التجارب السابقة الذكر يطبق نفسه في محرك رباعي الاسطوانات رباعي الاشواط من نوع (M-Zetor) وعند كل نوع من الوقود المستعمل. تم استخدام طريقة المصفوفات الانتقالية في هذه الدراسة لغرض تحليل النموذج الرياضي لعمود المرفق للمحرك المذكور أنفا مع الاخذ بنظر الاعتبار تأثير القص و التأثير الجايرسكوبي وقوى عدم الموازنة وكذلك تم الأخذ بنظر الاعتبار تمثيل طبقة الزيت للمحامل بمعاملين من المرونة والتخميد لكل كرسي تحميل.

تم بناء برامج حاسوبية بلغة فورتران لاحتضان الجانب النظري و التحليلي والتي يمكن من خلالها حساب الاستجابة الديناميكية لعمود المرفق .

لقد تبين من خلال نتائج البحث بانه عند اضافة 10% من الميثانول الى الوقود الاساسي (الكازولين) كنسبة حجمية يعطي افضل اهتزاز على طول عمود المرفق.